HHS Public Access

Author manuscript

Microbes Infect. Author manuscript; available in PMC 2021 October 01.

Published in final edited form as:

Microbes Infect. 2020 October ; 22(9): 423–431. doi:10.1016/j.micinf.2020.05.015.

Human Mesenchymal Stem Cell Based Intracellular Dormancy Model of *Mycobacterium tuberculosis*

Vipul K Singh[1], **Abhishek Mishra**[1], **Steven Bark**[2], **Arunmani Mani**[3], **Selvakumar Subbian**[4], **Robert L Hunter**[1], **Chinnaswamy Jagannath**[1], **Arshad Khan**[1,*]

[1]Department of Pathology and Genomic Medicine, Houston Methodist Research Institute, Houston TX 77030

[2]Department of Biology and Biochemistry, Science & Engineering Research Center, University of Houston, Houston, TX 77004

[3]Department of Obstetrics, Gynecology & Reproductive Sciences, McGovern Medical School, University of Texas Health Sciences Center-Houston, Houston TX 77030

[4]Department of Medicine, New Jersey Medical School, Public Health Research Institute, Newark, NJ 07103

Abstract

Understanding the biology of the tuberculosis pathogen during dormant asymptomatic infection, called latent tuberculosis is crucial to decipher a resilient therapeutic strategy for the disease. Recent discoveries exhibiting presence of pathogen's DNA and bacilli in mesenchymal stem cells (MSCs) of human and mouse despite completion of antitubercular therapy, indicates that these specific cells could be one of the niches for dormant *M. tuberculosis* in humans. To determine if *in vitro* infection of human MSCs could recapitulate the *in vivo* characteristics of dormant *M. tuberculosis,* we examined survival, phenotype, and drug susceptibility of the pathogen in MSCs. When a very low multiplicity of infection (1:1) was used, *M. tuberculosis* could survive in human bone marrow derived MSCs for more than 22 days without any growth. At this low level of infection, the pathogen did not cause any noticeable host cell death. During the later phase of infection, MSC-residing *M. tuberculosis* exhibited increased expression of HspX (a 16-kDa alpha-crystallin homolog) with a concurrent increase in tolerance to the frontline antitubercular drugs Rifampin and isoniazid. These results present a human MSC-based *intracelllular* model of *M. tuberculosis* infection to dissect the mechanisms through which the pathogen acquires and maintains dormancy in the host.

[*] *Correspondence should be directed to:* Arshad Khan, PhD, Assistant Professor, Department of Pathology and Genomic Medicine, Houston Methodist Research Institute, 6670 Bertner Ave, R6-330.7, Houston, TX 77030, Phone: 713.441-0704, Fax: 713.441.7295, akhan5@houstonmethodist.org.

Competing Interest Statement

Authors declare no financial or competing interest with any organization or personnel.

Keywords

Mycobacterium tuberculosis; Mesenchymal stem cells; Dormancy; Drug tolerance; Intracellular infection; Rifampin; Isoniazid

1. Introduction

Tuberculosis (TB) claims nearly 1.4 million lives annually and is the leading cause of death due to infection [1]. Although frontline drugs are available that can effectively control the disease, non-adherence to lengthy chemotherapy is one of the major causes of treatment failure. Because the etiological agent of TB, *Mycobacterium tuberculosis,* is able to survive in a dormant state for a long period of time in the presence of multiple antibiotics, it is imperative to adhere to a protracted treatment regimen [2,3]. Based on evidence from *in vitro* and animal models of TB, phenotypically different subpopulations of *M. tuberculosis* exist and contribute to the pathogen acquiring increased tolerance to antimicrobial drugs [4]. TB patients typically become sputum negative for *M. tuberculosis* culture within 14-21 days of drug administration, but the drug regimen needs to be adhered to for 6 months to rule out any relapses of disease. Based on this, it has been postulated that a drug-tolerant subpopulation of the bacilli could persist in tissues and cells that may not attain required optimum dose for killing the pathogen. Host-induced stresses within the tissue or cellular microenvironment could also induce the transition of the pathogen into the dormant, drug-resistant phenotype. Several of these host-induced stresses have been explored as potential factors for *in vitro* models of dormant TB to characterize the metabolic changes that confer drug tolerance [5–8]. However, it is difficult to accurately assess the physiology of the dormant *M. tuberculosis* bacilli from these *in vitro* culture-based models because they do not fully recapitulate the drug-tolerant phenotype observed in the human host [9,10]. Several animal-based experimental models of TB have also been explored to characterize the physiology of dormant *M. tuberculosis,* but do not truly represent a dormant infection and latent stage of disease as seen in humans, their natural host [11,12]. Even in the human host, localization of the pathogen within the host becomes arduous because of the difficulty in obtaining the specimens from the site of infection and ambiguity about different host cell populations harboring dormant *M. tuberculosis* bacilli.

Recently, the involvement of mesenchymal stem cells (MSCs) with dormant *M. tuberculosis* bacilli has been documented [13,14]. Live *M. tuberculosis* bacilli from bone marrow (BM)-derived MSCs were recovered from individuals even after completion of antitubercular drug therapy [15]. An earlier report also demonstrated the recruitment of MSCs to the site of *M. tuberculosis* infection in mice and their presence in human TB granulomas [16]. Isolation of viable *M. tuberculosis* bacilli from murine BM-MSCs after prolonged treatment with antitubercular drugs further demonstrated that MSCs potentially provide an antibiotic-protective niche for dormant *M. tuberculosis* bacilli [17]. Furthermore, *M. tuberculosis* DNA has been detected in BM-MSCs of latently-infected human donors, and there is clinical evidence of that *M. tuberculosis* containing CD271+ MSCs are hypoxic, a critical microenvironmental factor that is known to be associated with dormancy in the pathogen [18,19]. Taken together, these data prompted us to investigate the survival, bacterial

characteristics, and drug susceptibility of MSC residing *M. tuberculosis* after infection *in vitro.* Our results indicate that *in vitro* infection of MSCs leads to *M. tuberculosis* bacilli that resembles the drug-tolerant dormant state of the pathogen. This human MSC-based *intracellular* infection model could, therefore, be used as a platform to understand and delineate the host microenvironment and bacterial components involved in the transition and establishment of *M. tuberculosis* dormancy.

2. Materials and Methods

2.1 Ethics Statement

All methods using human and animal cells were carried out in accordance with relevant guidelines and regulations from the Institutional Review Board of the University of Texas Health Science Center-Houston. All experimental protocols were approved by the University of Texas Institutional Biosafety Committee (UTHSC-IBC) that sanctioned the study (HSC-MS-15-0548). Healthy donor-derived bone marrow was from commercial sources and deidentified subjects, and thus no informed consent was necessary for their use in the *in vitro* cell culture studies, per the institutional human subjects review committee.

2.2 Bacterial Culture

M. tuberculosis H37Rv (ATCC 27294), green fluorescent protein-expressing *M. tuberculosis* H37Rv (GFP *M. tuberculosis*) strain (Kind Gift From Dr. David N. McMurray College Station, TX) and *M. bovis* BCG (ATCC 35734) were grown in shaking (150rpm) culture condition in Middlebrook 7H9 broth (Difco, Becton Dickinson) supplemented with 0.05% (v/v) Tween 80 and Middlebrook AODC Enrichment (Becton Dickinson) to mid-log phase (OD 600 nm 0.6± 0.8) and reseeded into fresh medium 7 days before infection, as described previously [20]. Before use for MSC infection, bacterial cultures were washed three times in PBS and sonicated at 4 watts for 60 seconds using a sonicator (60 Sonic Dismembrator, Fisher Scientific) to prepare a uniform single cell suspension of bacteria.

2.3 Human Bone Marrow-Derived Mesenchymal Stem Cells

All methods and procedures using mesenchymal stem cells from human subjects were carried out in accordance with the procedures approved under protocols HSC-MS-15-0548 from the Institutional Review Board of the University of Texas Health Sciences Center-Houston. Human bone marrow (BM)-derived MSCs were isolated, cultivated, and characterized using density centrifugation and plastic adherence, according to protocols previously described [21]. To confirm the purity of cells, MSCs were screened for typical MSC spindle-like morphology, growth kinetics and then phenotyped with flow cytometry using the common markers that are expressed by MSCs (CD11b−, CD19−, CD34−, CD45−, HLA-DR−, CD73+, CD90+, CD105+) [22]. After purification and characterization MSCs were expanded by plating 1000 cells/cm^2 in 75 cm^2 flasks with 15 ml of culture medium that was consisted of α-minimal essential medium (α-MEM; Sigma Aldrich M4526) and 16% fetal bovine serum (Atlanta Biologicals). MSCs were then incubated until they became 70% confluent with medium replaced every alternate day. After expansion, adherent MSCs were washed and harvested with 0.25% trypsin/1 mM EDTA treatment (Life Technologies) for 5 min at 37°C and resuspended with fresh culture medium (α-MEM + 16% fetal bovine

serum, + 10 μg/mL penicillin + 5 μg/mL gentamicin). A drug-free medium was used for subsequent experiments in 6/24/96 well plates or 8-chamber slides.

2.4 Infection

For infection, bacteria were sonicated (4 watts, 60 seconds) to break bacterial aggregates and prepare a uniform suspension. The bacterial suspension was then diluted in serum-free medium for addition to MSCs at various MOI in 6/24/96 well plates. After 4 hrs of incubation, the medium was replaced with fresh alpha-MEM medium containing 16% FBS. For long-term infections, the medium was replaced on alternating days. Alamar Blue cell viability reagent (Life Technologies, DAL1025) was used to assess cell viability by adding the ready-to-use 1X solution to uninfected or *M. tuberculosis*-infected MSCs at various time points, followed by fluorescence measurement through fluorimeter per the manufacturer's protocol. Intracellular bacterial counts at various times post-infection were determined by CFU assay on 7H11 agar plates. Uninfected controls were included for all time points.

2.5 *Intracellular Monitoring of* M. tuberculosis *Morphology, Cell Wall Thickness, Mycobacterium tuberculosis proteins Rv1734, HspX and ESAT-6 and host lipids.*

MSCs were plated in 8-well slide chambers at a density of 5,000 cells/chamber and rested for one day in antibiotic-free medium (Alpha-MEM with 16% FBS). Sonicated single cell suspensions of GFP *M. tuberculosis* were added to MSCs at an MOI of 1:1. After 4 hrs incubation, the medium was replaced with fresh alpha-MEM (containing 16% FBS), and the medium was replaced alternate days. At the indicated time points, infection slides were washed 3X with PBS, followed by incubation with 4% formalin for 15 min to fix the cells. Anti-Rv1734 antibody (Abcam # 64785), anti-HspX (OriGene Technologies # AM60034PU-N, MD, USA) and anti-ESAT-6 (Abcam # 26246) were used to detect specific proteins of *M. tuberculosis* present within MSCs, followed by secondary staining with Texas-red conjugated anti-IgG. Before examining the cells under a fluorescent microscope, slides were rinsed with ice-cold methanol. Analysis and deconvolution of images were done using a Nikon-Eclipse-80i microscope fitted with NIS-Elements AR analysis. Intracellular lipids were stained using Nile Red staining kit (Abcam #228553) following the manufacturer's protocol and then examined by fluorescent microscopy.

2.6 *Detection of HspX Protein in* M. tuberculosis*-infected MSCs by Western Blot*

For detection of HspX in MSC-residing *M. tuberculosis,* whole cell lysates were resolved by 4-15% gradient SDS-PAGE gel and transferred to a nitrocellulose membrane at 100V for 2 hours [MiniTransBlot Cell (Bio-Rad)]. After blocking with 3% BSA, the membrane was incubated with a 1:100 dilution of anti-HspX monoclonal antibody (OriGene Technologies # AM60034PU-N, MD, USA) as primary antibody at 4 °C with shaking (100 rpm) overnight. After 5X washes (15 min each) with 1X PBS-T, 1:500 dilution of the polyclonal secondary antibody goat anti-mouse IgG conjugated with HRP (Abcam, Cambridge, UK) was added and incubated for 2 hrs at 4 °C followed by 5X washes with 1X PBS-T. The protein was detected by chemiluminescence using the Super-Signal 1 West Pico Chemiluminescent Substrate (Pierce Biotechnology, Rockford, IL) following the manufacturer's recommendations. GAPDH was used as loading control to determine if samples have been

loaded equally across all wells and confirms effective protein transfer during the western blot protocol.

2.7 *Intra-MSC* M. tuberculosis *Antibiotic Susceptibility Testing*

INH, RIF, EMB, and PZA were purchased from Sigma Aldrich, USA. The solutions of these standard drugs were prepared in sterile water/DMSO per the manufacturers' instructions. MSCs were plated at a concentration of 1×10^4 cells per well in 24-well tissue culture white plates and allowed to adhere overnight in alpha-MEM medium. For the infection, mid-log phase *M. tuberculosis* culture was washed 3X with PBS and sonicated for 60 seconds at 4 watts using a sonicator (60 Sonic Dismembrator, Fisher Scientific). The bacteria were then diluted in alpha-MEM and added to the MSCs at a concentration of 1×10^4 CFU/well. After 4 hrs of infection at 37°C in 5% CO_2, macrophages were washed 3X with alpha-MEM and 1 mL of the medium, with or without antimycobacterial drugs, was added to each well. The concentrations tested for each drug were 0.25x, 1x, 2.5x, 5x, 10x, and 20x MIC. Each drug concentration was tested in triplicate. Medium with and without antimycobacterial drugs was changed alternating days. The viability of *M. tuberculosis* within MSCs at different incubation time points, with and without antibiotic, was assessed by CFU enumeration as described previously [23]. Briefly, MSCs were lysed with 0.05% SDS, and various cell lysate dilutions in PBS were then spread onto Middlebrook 7H11 plates for CFU determination after 21 days of incubation at 37° C.

2.8 Statistics

For all statistical analyses, PRISM (Version 5, GraphPad, San Diego) software was used. Statistical analysis was performed with Paired two-tailed Student's t-test/one-way ANOVA with post-hoc analysis. P values <0.05 were considered significant. While calculating p values, Shapiro–Wilk normality test as well as Kolmogorov-Smirnov test was used to confirm that same sample followed a normal distribution of $p<0.05$.

3. Results

3.1 *M. tuberculosis* Survives in Human MSCs for an Extended Period without Affecting Host Cell Viability

Previous studies have demonstrated that both human and murine MSCs harbor persistent *M. tuberculosis* bacilli even after prolonged antimicrobial therapy [15,17]. Subsequent studies also indicated that the microenvironment of MSCs *in vivo* is permissive for *M. tuberculosis* bacilli to enter a state of dormancy [18,19]. To determine whether *M. tuberculosis* acquires a similar phenotype in an isolated population of human MSCs infected *in vitro,* we first examined the intracellular bacterial CFUs and host cell viability over time. BM-derived human MSCs were infected with virulent *M. tuberculosis* H37Rv at different multiplicity of infection (MOI), and bacterial and host cell survival were monitored over time. We found that infection of BM-MSCs at an MOI of 1:1 did not permit growth of the bacilli or result in any significant host cell death for at least 22 days (Figure 1A and 1B). Compared to human MSCs, infection of the human macrophage THP-1 showed a time-dependent increase in *M. tuberculosis* burden while also causing host cell death, even at a low MOI of 1:1 (Supplementary Figure 1A). Although no significant increase in bacterial load was evident

in MSCs until day 22 at higher MOIs of 1:5 and 1:10, increased host cell death was observed during the later stages of infection compared to uninfected cells. A significantly increased number of extracellular CFUs were recovered at MOI 1:5 and 1:10, compared to MOI 1:1, which did not show any discernible levels of extracellular bacteria in MSCs (Figure 1C). THP-1 cells, however, exhibited a much higher host cell death even at low MOI of 1:1 (Supplementary Figure 1B).

To determine if only virulent *M. tuberculosis* were able to survive in MSCs, BM-MSC were infected with *M. bovis* BCG, a non-pathogenic mycobacterial strain, at various MOIs. *M. bovis* BCG was unable to survive in BM-MSCs beyond day 7 (Figure 1D) and did not induce any significant BM-MSC cell death at any MOI examined (MOI 1:1 to 1:10, Supplementary Figure 2). These results indicate that at low levels of infection, virulent *M. tuberculosis* could survive in MSCs for a longer period in a non-proliferating state without affecting host cell viability.

3.2 Human MSC-residing *M. tuberculosis* Bacilli Gradually Alter Morphology, Decrease Metabolic Activity, and Express Antigens Associated with Dormant Stage Pathogen Survival

Because MSC-residing *M. tuberculosis* bacilli did not proliferate despite prolonged incubation, we next examined the phenotype of these bacteria, using a GFP-labeled strain of the pathogen [H37rv] for infection. GFP expression in this strain was directed by the acetamidase promoter which remained continually detectable during in vitro cultivation without addition of acetamide (a known inducer of the acetamidase promoter). We found that the bacilli that were unable to multiply in MSCs altered their morphology to become thicker in shape over time (Figure 2A). In comparison, actively replicating bacilli residing in human macrophages did not show such changes in morphology (Supplementary Figure 3). Interestingly, the intrinsic fluorescence of the MSC-residing GFP *M. tuberculosis* bacilli began to decrease after 14 days of incubation (Figure 2A). At day 22 post-infection, GFP *M. tuberculosis* bacilli were completely invisible in MSCs, indicating the possible transition of the pathogen into a state that has very low metabolic activity.

To further investigate if MSC-residing *M. tuberculosis* expresses dormancy-related genes, we examined the expression of bacterial protein Rv1734, which is located within the *dosR* regulon and induced during dormancy (20). Persistent expression of Rv1734 was seen in *M. tuberculosis*-infected MSCs during later phases of infection (Day 14-22), although a lower level of expression of this protein could also be observed during the early phase of infection (Day 1-7) (Figure 2B). Increased expression of Rv1734 also coincided with the shift of *M. tuberculosis* bacilli into a morphologically and metabolically altered phenotype. Conversely, expression of Rv1734 in *M. tuberculosis*-infected THP-1 macrophages was detected at neither stage of infection (Supplementary Figure 4). These results provide initial evidence that, because of the existence of a specific intracellular environment, *M. tuberculosis* bacilli residing in MSCs start transitioning into a dormant phenotype during the very early stages of infection. It is possible that the loss of GFP signal in the MSC residing *M. tuberculosis* bacilli at later stage of infection could be due to reduced activity of the specific gene that is driving the expression of the acetamidase reporter, rather than the low metabolic activity of

the pathogen at later stage of infection. We therefore examined the expression of *M. tuberculosis* virulent protein ESAT-6 in MSCs during early as well as later stage of infection. Expression of ESAT-6 was also lost during later stage of infection, which indicated that loss of GFP signal could be due to reduction in metabolic activity of *M. tuberculosis* bacilli during their transition to dormancy in MSCs (Fig 2D). THP-1 macrophages on the other hand had consistent expression of ESAT-6 during the infection (Supplementary Figure 5).

Because *M. tuberculosis* bacilli residing within MSCs developed thicker cell morphology over a period of time, we examined whether these changes were associated with alterations in the expression of bacterial cell wall-associated proteins. A 16-kDa alpha-crystallin homolog associated with the cell envelope of *M. tuberculosis* (HspX) has been reported to be involved in cell wall thickening during low oxygen tension-induced dormancy *in vitro* [24]. Bacteria were harvested from MSCs on the indicated days, and proteins were analyzed using Western blot with anti-HspX antibody. Expression of HspX was detected at day 7 and increased over time (Figure 2C). In contrast, expression of the HspX protein in human THP-1 macrophage cell line remained low over all time points analyzed (Supplementary Figure 6). These results indicate that the non-replicating pathogen residing in MSCs undergoes changes in arrangements of cell wall components that could have caused the alterations in overall cell morphology. These changes may help the pathogen to stabilize cell structures in preparation for long-term survival in human MSCs. Interestingly, we also found accumulation of Lipid Bodies (LBs) in *M. tuberculosis* infected MSCs though fusion between phagosomes and LB was not observed (Figure 2E). THP-1 macrophages on the other hand exhibited significantly lower levels of LB accumulation during *M. tuberculosis* infection (Supplementary Figure 7). Accumulation of LBs have also been shown to occur in foamy macrophages during the arrest of mycobacterial growth [25,26]. A similar phenomena in MSCs indicated that accumulation of LBs could be a common feature present in cells that harbor dormant *M. tuberculosis* bacilli.

3.3 *M. tuberculosis* Residing within MSCs Gradually Acquire Tolerance to First-Line Antimicrobials

Having observed that *M. tuberculosis* bacilli present in primary human MSCs were not proliferating and decreased their metabolic activity, we examined whether susceptibility of these bacteria to antimycobacterial drugs was also altered. To test this, first-line antitubercular drugs rifampin (RIF), isoniazid (INH), ethambutol (ETB), and pyrazinamide (PZA) were added immediately after infection at various concentrations spanning the spectrum of peak serum levels in humans, followed by time-dependent measurement of bacterial burden. MSCs were infected at low MOI (1:1), and time-kill kinetics of MSC-residing bacteria were then monitored by CFU assay. No significant bacterial killing was exerted by the first-line drugs EMB and PZA when they were added at the beginning of infection (Figure 3A). Between RIF and INH, only RIF could achieve complete elimination of *M. tuberculosis* bacilli from MSC, although this was only achieved after seven days of treatment at high doses, nearing concentrations equivalent to peak serum levels of patients undergoing chemotherapy [27]. Although INH achieved significant bacterial killing of intra-MSC *M. tuberculosis,* it could not achieve complete elimination of the bacilli even at concentrations 25-50 times higher than the known minimum bactericidal concentration

(MBC) of the drug against the virulent H37Rv strain in human macrophages (Figure 3A) [28].

Because *M. tuberculosis* bacilli gradually increased cell thickness and lost metabolic activity over time during residence in MSCs, we next examined the susceptibility of bacteria to first-line antitubercular drugs when they were added at later stages of infection. In this experiment, RIF, INH, ETB, and PZA were added 7 and 14 days post-infection and intracellular bacterial load was measured at various days post-treatment. We found that only RIF could attain significant killing of *M. tuberculosis* bacilli within MSCs, whereas none of the other three drugs had any bactericidal effect when added at later stages of infection (Figure 3B and C). Nonetheless, tolerance of MSC-residing *M. tuberculosis* to the RIF was also increased during the later stage of infection, as it could not eliminate the infection even after 8 days of treatment and with a dose equivalent to peak human serum levels. Because antitubercular drugs are known to work optimally when used in tandem with each other, we further examined the killing effect of drugs when they were applied together to intra-MSC *M. tuberculosis.* While a moderate synergistic effect of anti-TB drugs was observed when they were added at the beginning of infection, the addition of the antimicrobials at day 7 and day 14 post-infection exhibited a similar drug tolerance profile seen when these drugs were added alone to intra-MSC *M. tuberculosis* (Figure 3D). Increased tolerance of MSC-residing *M. tuberculosis* to RIF and INH during later stages of infection thus clearly indicated that in these specialized stem cells, the pathogen gradually attains increased tolerance to antibiotics, a phenotype that has been associated with dormant bacilli.

4. Discussion

Characteristics features of *M. tuberculosis* dormancy as seen in humans is not recapitulated in any available animal models, and a more robust system is needed to study and understand the natural course of infection and disease progression [11]. Studying dormancy in human subjects *in vivo* is extremely challenging because of the difficulties in obtaining specimens from asymptomatic subjects and unknown niches that potentially harbor dormant bacteria. *In vitro* studies of dormancy in human cells, such as macrophages and dendritic cells, that have been suggested to be involved in harboring the *M. tuberculosis* bacilli fail to recreate the dormancy phenotype of the pathogen [9,29]. Although various stress-induced axenic culture-based dormancy models of *M. tuberculosis* have been developed and characterized in some detail, it is difficult to establish if they truly represent the phenotype of the pathogen that exists in their host *in vivo* [30].

In this study, the natural ability of MSCs to control infection for a long period provides the first proof of non-proliferative dormant-like behavior of *M. tuberculosis* in a human host cell (Figure 1A and 1C). Although containment of infection, which also did not result in any discernible harm to host cells, was only seen at lower MOI, the natural course of infection in humans is also known to be caused by exposure to a very low number of bacilli. The likelihood of *M. tuberculosis* infection resulting in active disease is suggested to be directly proportional to the infection inoculum and virulence of the strain [31,32]. This is because infection of phagocytic cells with a larger inoculum of a more virulent strain results in host cell death and thus dissemination of the pathogen. Infection of macrophages at low MOI

does not cause any significant host cell death until day 6 when the intracellular bacterial load reached a threshold level after *M. tuberculosis* replication [33]. At low MOI, the inability of *M. tuberculosis* to cause cell death with a negligible presence of extracellular bacilli and no increase in intracellular CFUs over 22 days, clearly indicates that *M. tuberculosis* replication was restricted in MSCs (Figure 1, A–C). These results provide evidence that perhaps intracellular environment within MSCs may not be conducive for the replication of *M. tuberculosis* and hence these specialized cells could be used to characterize the unique microenvironment that drives the pathogen into dormancy.

An earlier study by Cunningham et al. found that when *M. tuberculosis* is subjected to microaerophilic or anaerobic conditions, the bacilli develop strikingly thickened cell walls [24]. Because reduced oxygen tension is also known to trigger dormancy in *M. tuberculosis,* it has been suggested that increased cell wall thickness could help the bacilli survive for extended periods in a quiescent state. Nonetheless, the molecular mechanisms inducing such changes in bacterial cell wall morphology during intracellular survival have not been thoroughly investigated. The discovery of a suitable *in vitro* intracellular *M. tuberculosis* infection model that induces the dormant phenotype (Figure 2) could greatly facilitate such characterizations. Indeed, it has been determined that the intracellular MSC environment harboring *M. tuberculosis* is hypoxic; it will be interesting to determine if there are other MSC-specific intracellular factors that contribute to transitioning the pathogen into dormancy [18]. Hypoxia within MSC could be one of the driving factors for the induction of dormancy in *M. tuberculosis* during this long-term intracellular survival. Apart from the cell wall, altered morphology of dormant mycobacterial bacilli has also been reported in other studies, though only in an axenic culture-based dormancy model of TB. Dormancy induced by nutrient depletion in an *M. smegmatis* infection caused the bacteria to undergo a gradual transformation of rod-shaped bacilli into ovoid bacilli [34].

Although this study demonstrated the distinct morphology of dormant bacilli in a non-pathogenic mycobacteria strain, microscopic examination of *M. tuberculosis*-infected guinea pigs in organ homogenates also revealed the presence of denser and smaller bacterial forms with a rounded shape that persisted in animals even after completion of anti-TB therapy [39]. *M. tuberculosis* bacilli residing in MSCs also showed a similar trend of increasing bacterial cell density and reduction in cell size over time, although the shape of the bacilli was curved rather than ovoid (Figure 2A). Because earlier animal-based studies showed a more dramatic reduction in the size of the bacilli after incubation times of few months, a similar trend exhibited by *M. tuberculosis* within MSCs in a relatively short period could indicate the early phase of the dormancy in these specific cells (Figure 2A). In *M. tuberculosis*-infected guinea pigs that had undergone antimicrobial treatment, viable *M. tuberculosis* bacilli from organ homogenates could no longer be detected through standard plating procedures, but MSC-residing organisms were able to form colonies on agar plates [39], suggesting that the pathogen persisting in MSCs could yet be in the transition state. Previous studies suggest that re-modelling of cell wall occurs during the establishment of dormancy in *M. tuberculosis* [35,36]. While cell wall peptidoglycan of actively replicating *M. tuberculosis* has been shown to contain a network of classical 3 - 4 transpeptide bonds, peptidoglycan from non-replicating bacilli contained significantly more non-classical 3 - 3 linkages. Since we observed increased production of HspX (Figure 2C) that is known to be

associated with cell envelope of *M. tuberculosis,* molecular rearrangement in the peptidoglycan layer through non-classical 3 - 3 transpeptide linkages could perhaps help the pathogen to accommodate more HspX in its cell wall during shift into dormancy. Shedding of mycolates and lipoglycans along with increased arabinosylation has also been shown to cause changes in Mycobacterial cell wall during non-replicating persistence in dormant state [35,37,38]. Al these rearrangements in cell wall hence could be the causative factors for changes that occur in the overall morphology of *M. tuberculosis* during dormancy and having critical implications for the survival of the pathogen in non- replicating state. A steady reduction in metabolic activity as demonstrated by loss of fluorescence from the GFP-tagged *M. tuberculosis* also suggests the gradual transition of the bacilli into a state of dormancy (Figure 2A,B,C and D). Low metabolic activity of dormant *M. tuberculosis* has been reported in other culture-based dormancy models, but remained unexamined in an intracellular infection model [40]. Overall, based on the morphological changes and reduction in metabolic activity of MSC-residing *M. tuberculosis* over time that were observed in other animal and culture dormancy models, we suggest that transition of the pathogen towards dormancy could also occur in the intracellular environment. Human MSCs have been indeed shown to exhibit direct as well as indirect antimicrobial activity in vitro against a variety of other bacterial pathogens including *Pseudomonas aeruginosa, Staphylococcus aureus,* and *Streptococcus pneumonia,* through the secretion of antimicrobial peptide LL-37 and induction of host innate responses [41,42]. However, it still remains to be determined if MSCs can restrict and control the bacterial growth of other intracellular pathogens in a fashion similar to *M. tuberculosis.*

Increased tolerance of dormant *M. tuberculosis* bacilli to antibiotics has been suggested based on the persistence of the pathogen despite long chemotherapy courses in humans and experimental animal models of TB [4,43]. However, the drug tolerance/resistance phenotype of *M. tuberculosis* in a true dormancy model remains to be characterized. Available axenic culture-based dormancy models of TB do not depict a uniform population of *M. tuberculosis* that can exhibit resistance or tolerance to antitubercular drugs for an extended period. Additionally, a large discrepancy has been observed in the susceptibility of axenic cultures versus the intracellular cultures of *M. tuberculosis,* in which intracellular bacilli appear to be more tolerant of antibiotics for longer periods [20,44]. In this study, we observed that after extended incubation within MSCs, *M. tuberculosis* could significantly increase its tolerance to the most effective first-line antitubercular drugs INH and RIF (Figure 3).

The bacterial components that results in a drug-tolerant phenotype in *M. tuberculosis* during the dormant stage remains unclear. Using MSC based intracellular dormancy model, a global transcriptome and proteome profile of macrophage- vs. MSC-residing *M. tuberculosis* could be compared to delineate the specific molecular mechanisms that are involved in achieving drug tolerance during dormancy. Because we observed a correlation between increased bacterial cell thickening and drug tolerance, it will also be interesting to examine whether the cell wall structure of MSC-residing *M. tuberculosis* differs compared to macrophage-residing organisms. One possibility is that altered cell wall organization could contribute to changes in cell wall permeability and thus drug tolerance. The efflux pumps present in bacteria and host cells may also contribute to drug tolerance, as has been suggested by some recent studies [45].

In summary, we observed a non-proliferative dormant-like phenotype of *M. tuberculosis* in human MSCs, and propose that these specialized cells could be a useful *in vitro* model for dissecting the host and bacterial events that occur during the transition, and/or maintenance of dormancy. Elucidation of bacterial components involved in resistance against host defenses could greatly facilitate the discovery of host-directed interventions and strategies to eliminate dormant bacilli. Dissecting the bacterial pathways that are essential for the maintenance of intracellular dormancy, and are involved in conferring drug resistance to the pathogen, could help identify vital drug targets and the development of novel antimicrobials to kill dormant *M. tuberculosis.*

Supplementary Material

Refer to Web version on PubMed Central for supplementary material.

Acknowledgments

We thank Dr. Jeffrey Actor, Professor, McGovern Medical School, University of Texas Health Science Center-Houston for technical assistance with this project and Dr. Shen-An Hwang, Assistant Professor, McGovern Medical School, University of Texas Health Science Center-Houston for comments that greatly helped in the compilation of the manuscript.

References

[1]. Zumla A, Oliver M, Sharma V, Masham S, Herbert N. World TB Day 2016--advancing global tuberculosis control efforts. Lancet Infect Dis 2016;16:396–8. doi:10.1016/S1473-3099(16)00086-4. [PubMed: 27036334]

[2]. Zhang Y, Yew WW, Barer MR. Targeting persisters for tuberculosis control. Antimicrob Agents Chemother 2012;56:2223–30. doi:10.1128/AAC.06288-11. [PubMed: 22391538]

[3]. Connolly LE, Edelstein PH, Ramakrishnan L. Why is long-term therapy required to cure tuberculosis? PLoS Med 2007;4:e120. doi:10.1371/journal.pmed.0040120. [PubMed: 17388672]

[4]. Evangelopoulos D, Fonseca JD da, Waddell SJ. Understanding anti-tuberculosis drug efficacy: rethinking bacterial populations and how we model them. Int J Infect Dis 2015;32:76–80. doi:10.1016/j.ijid.2014.11.028. [PubMed: 25809760]

[5]. Sarathy J, Dartois V, Dick T, Gengenbacher M. Reduced Drug Uptake in Phenotypically Resistant Nutrient-Starved Nonreplicating Mycobacterium tuberculosis. Antimicrob Agents Chemother 2013;57:1648–53. doi:10.1128/AAC.02202-12. [PubMed: 23335744]

[6]. Turapov O, O'Connor BD, Sarybaeva AA, Williams C, Patel H, Kadyrov AS, et al. Phenotypically Adapted Mycobacterium tuberculosis Populations from Sputum Are Tolerant to First-Line Drugs. Antimicrob Agents Chemother 2016;60:2476–83. doi:10.1128/AAC.01380-15. [PubMed: 26883695]

[7]. Deb C, Lee C-M, Dubey VS, Daniel J, Abomoelak B, Sirakova TD, et al. A Novel In Vitro Multiple-Stress Dormancy Model for Mycobacterium tuberculosis Generates a Lipid-Loaded, Drug-Tolerant, Dormant Pathogen. PLoS One 2009;4:e6077. doi:10.1371/journal.pone.0006077. [PubMed: 19562030]

[8]. Wayne LG, Sohaskey CD. Nonreplicating persistence of mycobacterium tuberculosis. Annu Rev Microbiol 2001 ;55:139–63. doi: 10.1146/annurev.micro.55.1.139. [PubMed: 11544352]

[9]. Jhamb S, Singh P, Patel K. Models of latent tuberculosis: Their salient features, limitations, and development. J Lab Physicians 2011;3:75. doi:10.4103/0974-2727.86837. [PubMed: 22219558]

[10]. Alnimr AM. Dormancy models for <italic>Mycobacterium tuberculosis</italic>: A minireview. Brazilian J Microbiol 2015;46:641–7. doi:10.1590/S1517-838246320140507.

[11]. Gupta UD, Katoch VM. Animal models of tuberculosis. Tuberculosis (Edinb) n.d.;85:277–93. doi:10.1016/j.tube.2005.08.008.

[12]. Lin PL, Kirschner D, Flynn JL. Modeling pathogen and host: in vitro, in vivo and in silico models of latent Mycobacterium tuberculosis infection. Drug Discov Today Dis Model 2005;2:149–54. doi:10.1016/j.ddmod.2005.05.019.

[13]. Khan A, Hunter RL, Jagannath C. Emerging role of mesenchymal stem cells during tuberculosis: The fifth element in cell mediated immunity. Tuberculosis 2016;101:S45–52. doi:10.1016/j.tube.2016.09.019.

[14]. Khan A, Mann L, Papanna R, Lyu MA, Singh CR, Olson S, et al. Mesenchymal stem cells internalize Mycobacterium tuberculosis through scavenger receptors and restrict bacterial growth through autophagy. Sci Rep 2017;7. doi:10.1038/s41598-017-15290-z. [PubMed: 28127057]

[15]. Das B, Kashino SS, Pulu I, Kalita D, Swami V, Yeger H, et al. CD271+ Bone Marrow Mesenchymal Stem Cells May Provide a Niche for Dormant Mycobacterium tuberculosis. Sci Transl Med 2013;5:170ra13–170ra13. doi:10.1126/scitranslmed.3004912.

[16]. Raghuvanshi S, Sharma P, Singh S, Van Kaer L, Das G. Mycobacterium tuberculosis evades host immunity by recruiting mesenchymal stem cells. Proc Natl Acad Sci 2010;107:21653–8. doi:10.1073/pnas.1007967107. [PubMed: 21135221]

[17]. Beamer G, Major S, Das B, Campos-Neto A. Bone marrow mesenchymal stem cells provide an antibiotic-protective niche for persistent viable Mycobacterium tuberculosis that survive antibiotic treatment. Am J Pathol 2014;184:3170–5. doi:10.1016/j.ajpath.2014.08.024. [PubMed: 25451154]

[18]. Garhyan J, Bhuyan S, Pulu I, Kalita D, Das B, Bhatnagar R. Preclinical and Clinical Evidence of Mycobacterium tuberculosis Persistence in the Hypoxic Niche of Bone Marrow Mesenchymal Stem Cells after Therapy. Am J Pathol 2015;185:1924–34. doi:10.1016/j.ajpath.2015.03.028. [PubMed: 26066709]

[19]. Tornack J, Reece ST, Bauer WM, Vogelzang A, Bandermann S, Zedler U, et al. Human and Mouse Hematopoietic Stem Cells Are a Depot for Dormant Mycobacterium tuberculosis. PLoS One 2017;12:e0169119. doi:10.1371/journal.pone.0169119. [PubMed: 28046053]

[20]. Chanwong S, Maneekarn N, Makonkawkeyoon L, Makonkawkeyoon S. Intracellular growth and drug susceptibility of Mycobacterium tuberculosis in macrophages. Tuberculosis (Edinb) 2007;87:130–3. doi:10.1016/j.tube.2006.06.001. [PubMed: 16860611]

[21]. Sekiya I, Larson BL, Smith JR, Pochampally R, Cui J-G, Prockop DJ. Expansion of human adult stem cells from bone marrow stroma: conditions that maximize the yields of early progenitors and evaluate their quality. Stem Cells 2002;20:530–41. doi:10.1634/stemcells.20-6-530. [PubMed: 12456961]

[22]. Mosna F, Sensebé L, Krampera M. Human bone marrow and adipose tissue mesenchymal stem cells: a user's guide. Stem Cells Dev 2010;19:1449–70. doi:10.1089/scd.2010.0140. [PubMed: 20486777]

[23]. de Steenwinkel JEM, de Knegt GJ, ten Kate MT, van Belkum A, Verbrugh HA, Kremer K, et al. Time-kill kinetics of anti-tuberculosis drugs, and emergence of resistance, in relation to metabolic activity of Mycobacterium tuberculosis. J Antimicrob Chemother 2010;65:2582–9. doi: 10.1093/jac/dkq374. [PubMed: 20947621]

[24]. Cunningham AF, Spreadbury CL. Mycobacterial stationary phase induced by low oxygen tension: cell wall thickening and localization of the 16-kilodalton alpha-crystallin homolog. J Bacteriol 1998;180:801–8. [PubMed: 9473032]

[25]. Caire-Brändli I, Papadopoulos A, Malaga W, Marais D, Canaan S, Thilo L, et al. Reversible Lipid Accumulation and Associated Division Arrest of Mycobacterium avium in Lipoprotein-Induced Foamy Macrophages May Resemble Key Events during Latency and Reactivation of Tuberculosis. Infect Immun 2014;82:476–90. doi:10.1128/IAI.01196-13. [PubMed: 24478064]

[26]. Daniel J, Maamar H, Deb C, Sirakova TD, Kolattukudy PE. Mycobacterium tuberculosis Uses Host esTriacylglycerol to Accumulate Lipid Droplets and Acquires a Dormancy-Like Phenotype in Lipid-Loaded Macrophag. PLoS Pathog 2011;7:e1002093. doi:10.1371/journal.ppat.1002093. [PubMed: 21731490]

[27]. Park JS, Lee J-Y, Lee YJ, Kim SJ, Cho Y-J, Yoon H Il, et al. Serum Levels of Antituberculosis Drugs and Their Effect on Tuberculosis Treatment Outcome. Antimicrob Agents Chemother 2016;60:92–8. doi:10.1128/AAC.00693-15. [PubMed: 26459901]

[28]. Rastogi N, Labrousse V, Goh KS. In Vitro Activities of Fourteen Antimicrobial Agents Against Drug Susceptible and Resistant Clinical Isolates of Mycobacterium tuberculosis and Comparative Intracellular Activities Against the Virulent H37Rv Strain in Human Macrophages. Curr Microbiol 1996;33:167–75. doi:10.1007/s002849900095. [PubMed: 8672093]

[29]. Tailleux L, Neyrolles O, Honore-Bouakline S, Perret E, Sanchez F, Abastado J-P, et al. Constrained Intracellular Survival of Mycobacterium tuberculosis in Human Dendritic Cells. J Immunol 2003;170:1939–48. doi:10.4049/jimmunol.170.4.1939. [PubMed: 12574362]

[30]. Dutta NK, Karakousis PC. Latent Tuberculosis Infection: Myths, Models, and Molecular Mechanisms. Microbiol Mol Biol Rev 2014;78:343–71. doi:10.1128/MMBR.00010-14. [PubMed: 25184558]

[31]. Fennelly KP, Jones-López EC. Quantity and Quality of Inhaled Dose Predicts Immunopathology in Tuberculosis. Front Immunol 2015;6. doi:10.3389/fimmu.2015.00313.

[32]. Repasy T, Lee J, Marino S, Martinez N, Kirschner DE, Hendricks G, et al. Intracellular bacillary burden reflects a burst size for Mycobacterium tuberculosis in vivo. PLoS Pathog 2013;9:e1003190. doi:10.1371/journal.ppat.1003190. [PubMed: 23436998]

[33]. Lee J, Repasy T, Papavinasasundaram K, Sassetti C, Kornfeld H. Mycobacterium tuberculosis Induces an Atypical Cell Death Mode to Escape from Infected Macrophages. PLoS One 2011;6:e18367. doi:10.1371/journal.pone.0018367. [PubMed: 21483832]

[34]. Anuchin AM, Mulyukin AL, Suzina NE, Duda VI, El-Registan GI, Kaprelyants AS. Dormant forms of Mycobacterium smegmatis with distinct morphology. Microbiology 2009;155:1071–9. doi: 10.1099/mic.0.023028-0. [PubMed: 19332809]

[35]. Bacon J, Alderwick LJ, Allnutt JA, Gabasova E, Watson R, Hatch KA, et al. Non-Replicating Mycobacterium tuberculosis Elicits a Reduced Infectivity Profile with Corresponding Modifications to the Cell Wall and Extracellular Matrix. PLoS One 2014;9:e87329. doi:10.1371/journal.pone.0087329. [PubMed: 24516549]

[36]. Alderwick LJ, Harrison J, Lloyd GS, Birch HL. The Mycobacterial Cell Wall Peptidoglycan and Arabinogalactan. Cold Spring Harb Perspect Med 2015;5:a021113. doi: 10.1101/cshperspect.a021113. [PubMed: 25818664]

[37]. Deb C, Lee C-M, Dubey VS, Daniel J, Abomoelak B, Sirakova TD, et al. A Novel In Vitro Multiple-Stress Dormancy Model for Mycobacterium tuberculosis Generates a Lipid-Loaded, Drug-Tolerant, Dormant Pathogen. PLoS One 2009;4:e6077. doi:10.1371/journal.pone.0006077. [PubMed: 19562030]

[38]. Caño-Muñiz S, Anthony R, Niemann S, Alffenaar J-WC. New Approaches and Therapeutic Options for Mycobacterium tuberculosis in a Dormant State. Clin Microbiol Rev 2017;31. doi:10.1128/CMR.00060-17.

[39]. WERNER GH. Filterable forms of mycobacterium tuberculosis. Am Rev Tuberc 1954;69:473–4. [PubMed: 13138882]

[40]. Bacon J, Alderwick LJ, Allnutt JA, Gabasova E, Watson R, Hatch KA, et al. Non-Replicating Mycobacterium tuberculosis Elicits a Reduced Infectivity Profile with Corresponding Modifications to the Cell Wall and Extracellular Matrix. PLoS One 2014;9:e87329. doi:10.1371/journal.pone.0087329. [PubMed: 24516549]

[41]. Chow L, Johnson V, Impastato R, Coy J, Strumpf A, Dow S. Antibacterial activity of human mesenchymal stem cells mediated directly by constitutively secreted factors and indirectly by activation of innate immune effector cells. Stem Cells Transl Med 2019:sctm.19-0092. doi: 10.1002/sctm.19-0092.

[42]. Sutton MT, Fletcher D, Ghosh SK, Weinberg A, van Heeckeren R, Kaur S, et al. Antimicrobial Properties of Mesenchymal Stem Cells: Therapeutic Potential for Cystic Fibrosis Infection, and Treatment. Stem Cells Int 2016;2016:1–12. doi:10.1155/2016/5303048.

[43]. Gengenbacher M, Kaufmann SHE. Mycobacterium tuberculosis: success through dormancy. FEMS Microbiol Rev 2012;36:514–32. doi:10.1111/j.1574-6976.2012.00331.x. [PubMed: 22320122]

[44]. Hartkoorn RC, Chandler B, Owen A, Ward SA, Bertel Squire S, Back DJ, et al. Differential drug susceptibility of intracellular and extracellular tuberculosis, and the impact of P-glycoprotein. Tuberculosis (Edinb) 2007;87:248–55. doi:10.1016/j.tube.2006.12.001. [PubMed: 17258938]

[45]. Szumowski JD, Adams KN, Edelstein PH, Ramakrishnan L. Antimicrobial efflux pumps and Mycobacterium tuberculosis drug tolerance: evolutionary considerations. Curr Top Microbiol Immunol 2013;374:81–108. doi:10.1007/82_2012_300. [PubMed: 23242857]

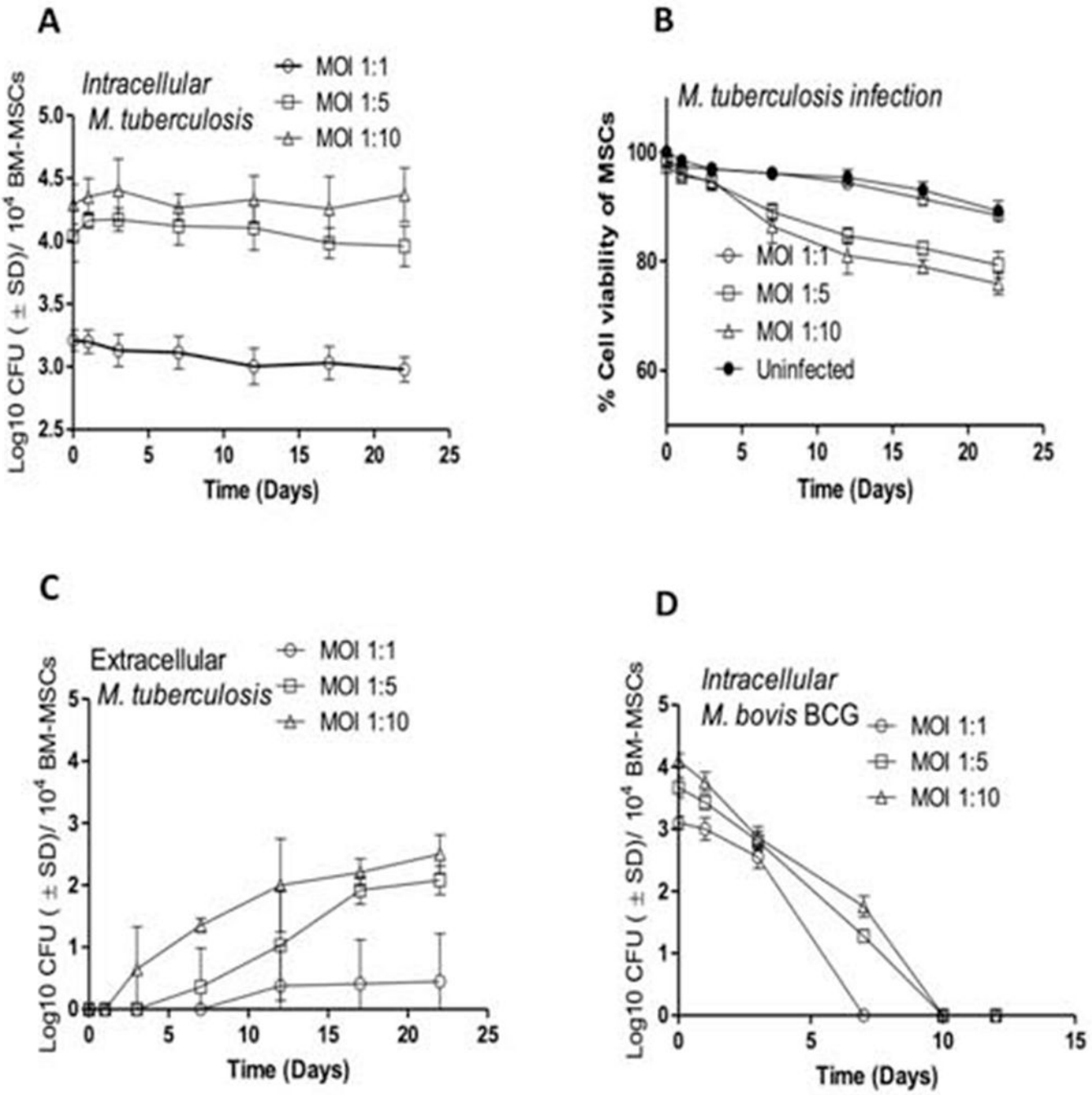

Figure 1.

Kinetics of bacterial burden and host cell viability of naïve human MSCs infected with *M. tuberculosis* and *M. bovis* BCG. **(A)** Growth and survival of *M. tuberculosis* bacilli within naïve human BM-MSCs over a period of 22 days when infected at various MOIs. **(B)** The viability of *M. tuberculosis*-infected MSCs over a period of 22 days when infected at various MOIs. **(C)** Extracellular bacilli present in *M. tuberculosis*-infected naïve human BM-MSCs over a period of 22 days at various MOIs **(D)** Growth and survival of *M. bovis* BCG within naïve human BM-MSCs over a period of 12 days when infected at various MOIs. Open

circles, MOI 1:1; open squares, MOI 1:5; open triangles, MOI 1:10; close circles, uninfected control. Bacterial burden was measured by CFU assay and cell viability was determined by Alamar Blue assay as described in Materials and Methods. Data are representative of 3 independent experiments (using MSCs from 3 different donors) carried out in duplicate and values are expressed as mean ± SD.

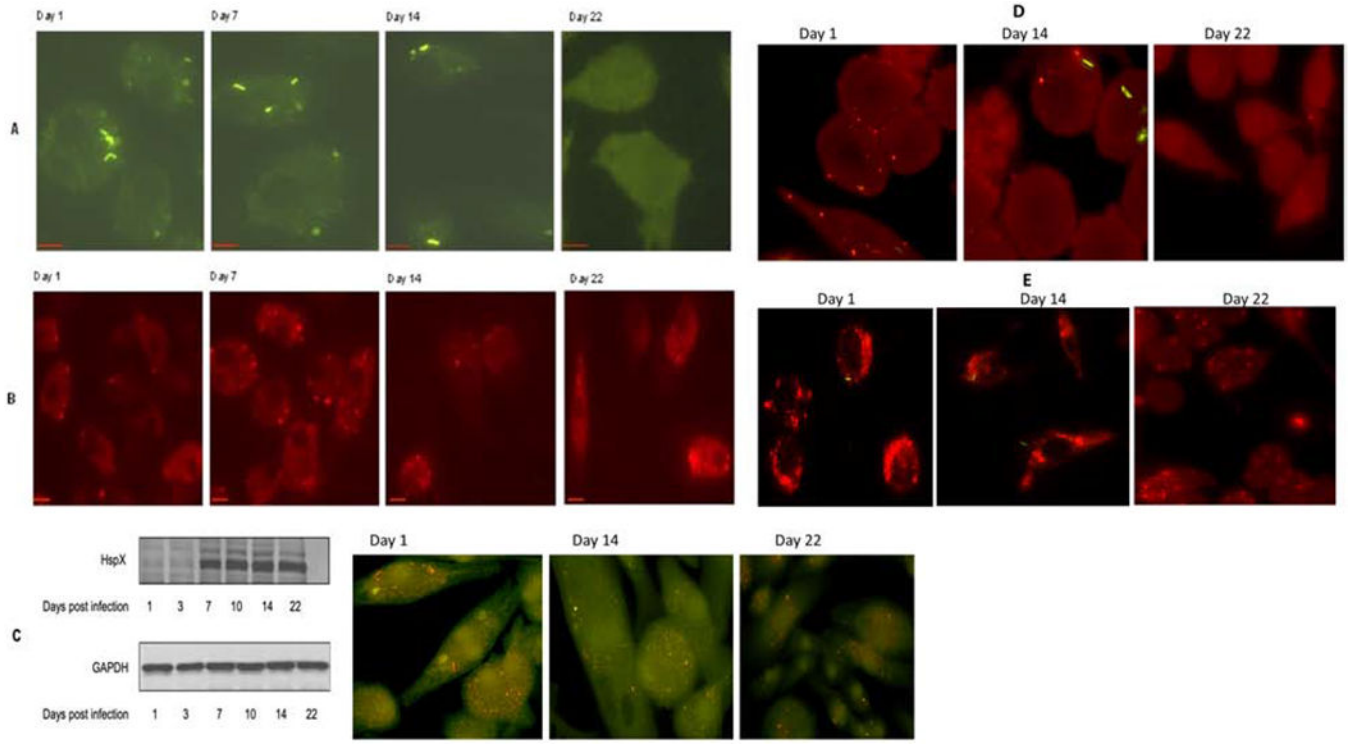

Figure 2.

M. tuberculosis undergoes time-dependent changes in morphology and metabolic activity in response to incubation in MSCs. **(A)** Fluorescent images of GFP-labeled *M. tuberculosis* within human MSCs at the indicated time points post-infection. **(B)** Time-dependent expression of *M. tuberculosis* dormancy antigen Rv1734 during its residence within human MSCs. For **(A)** and **(B)**: MSCs were infected at an MOI of 1:1 for 4 hrs. Time in days post-infection is indicated for all panels. Scale bars in the left corner of each image = 10 μm. Representative microscopy images from at least three independent experiments for each time point are shown. Fluorescent images were deconvolved using Nikon microscope's NIS-Element AR software. For each time point at least 15 separate high-power fields per sample were evaluated, per 3 experimental replicates. **(C)** Expression of cell wall-associated *M. tuberculosis* antigen HspX by western blot and intracellular staining at the indicated time points post infection; GADPH was used as a loading control for western blot. **(D)** Expression of ESAT-6 protein of *M. tuberculosis* within MSCs at different time post infection as detected by intracellular staining through fluorescent microscopy. **(E)** Accumulation of lipid bodies (Red) within MSCs at different time post infection with *M. tuberculosis* H37rv (Green). At selected time points, LB formation was monitored with Nile red that stains neutral lipids within cells.

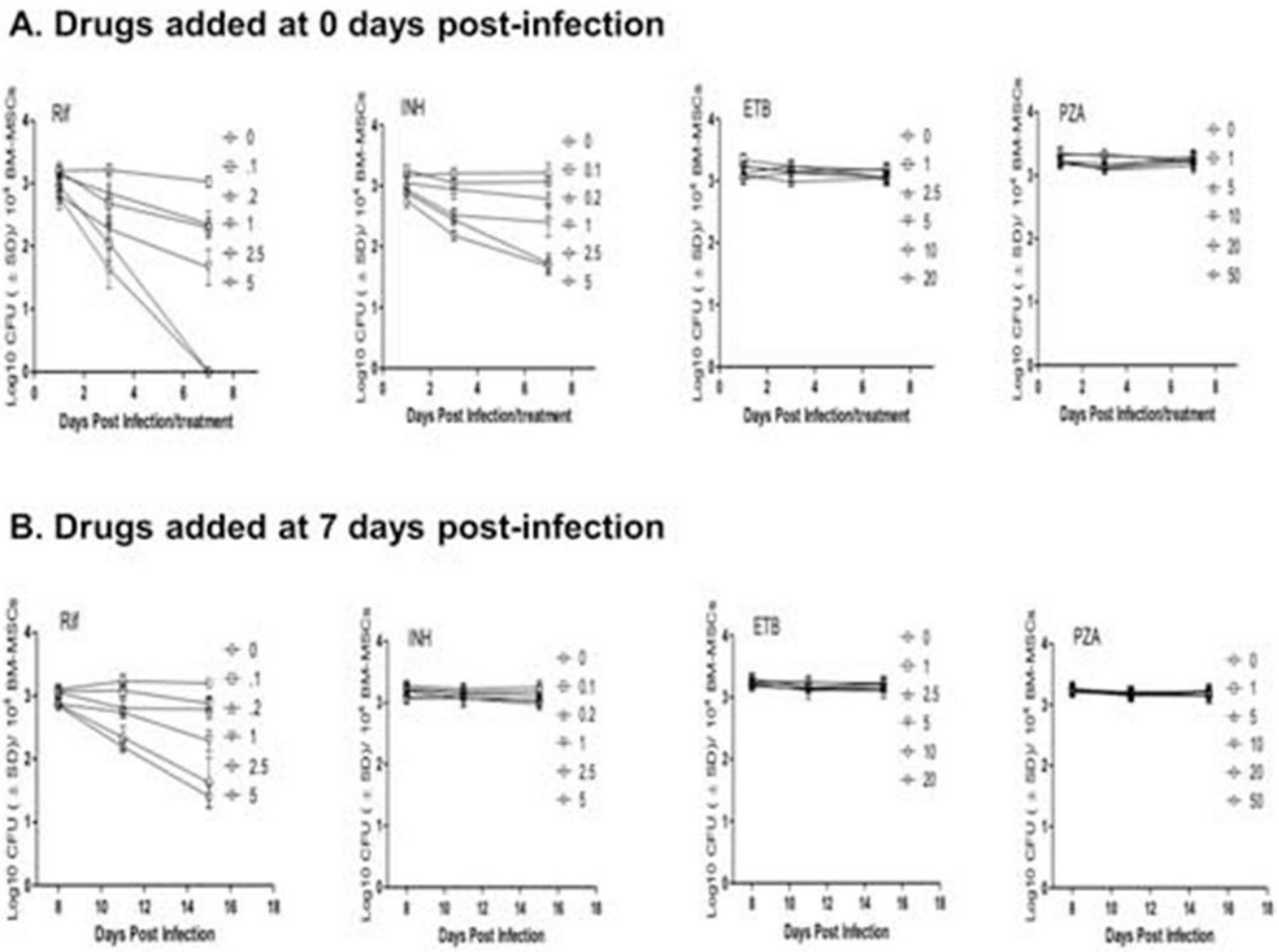

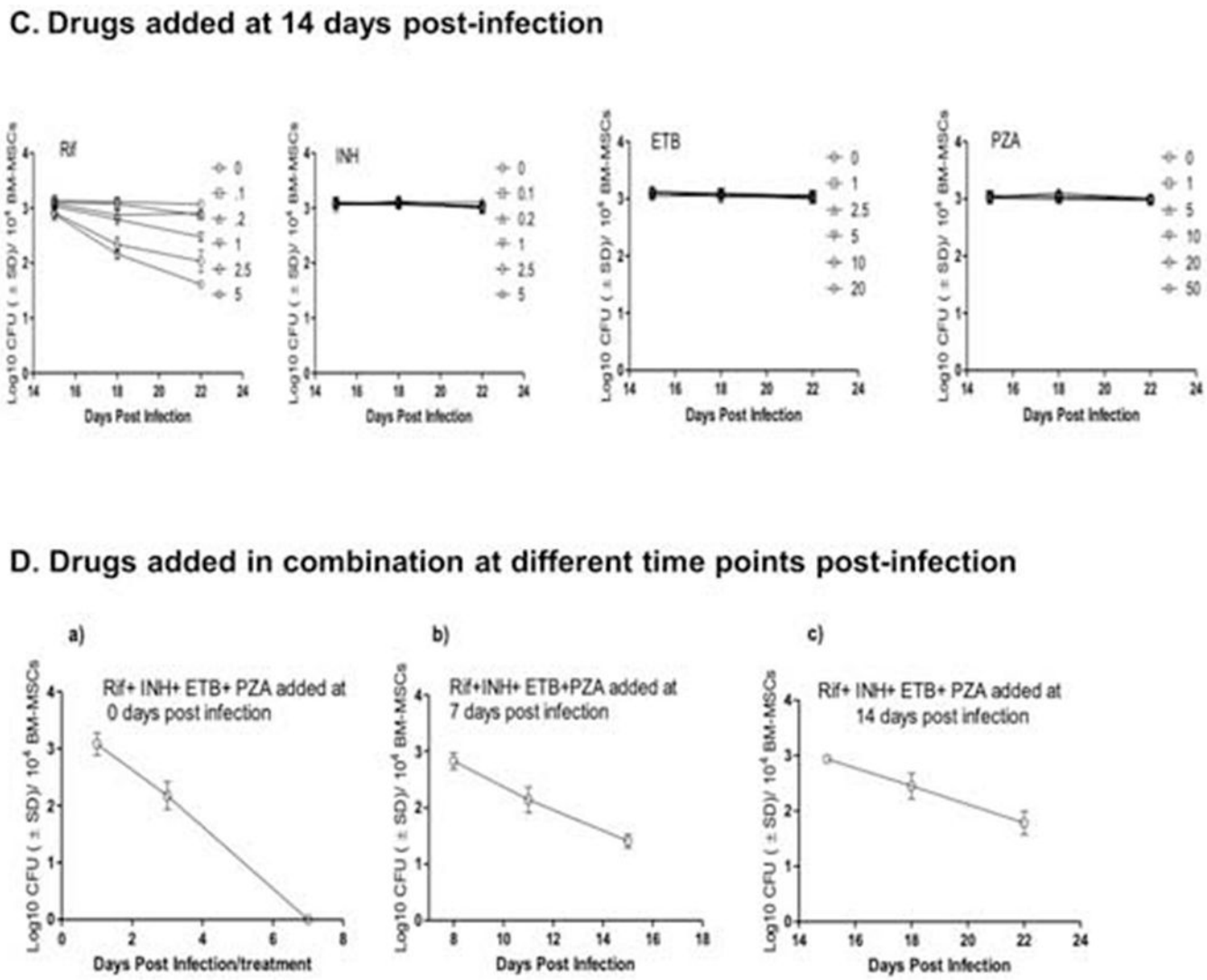

Figure 3.

Antibiotic susceptibility of intra-MSC *M. tuberculosis.* Dose-dependent killing kinetics of *M. tuberculosis* by first line antitubercular drugs Rifampin (RIF), isoniazid (INH), ethambutol (ETB) and pyrazinamide (PZA) when added alone at Day 0 **(A)**, Day 7 **(B)**, and Day 14 **(C)** post-infection. The effects of RIF, INH, ETB, and PZA at single doses of 2.5, 5, 10, and 20 μg/mL, and when added together is also shown **(D)**. MSCs were infected at MOI 1:1. Various doses of drugs shown in legends are in microgram/well/10^4 BM-MSCs. Culture medium and/or drugs were replaced every alternate day. Significant differences between treated samples and untreated controls were determined using 2-way ANOVA followed by Bonferroni's post-hoc test (indicated with asterisks). Data are representative of 3 independent experiments (using MSCs from 3 different donors) carried out in duplicate. Bars and error bars represent means and SD, respectively.